

# Study of High-Transverse-Momentum Higgs Boson Production in Association with a Vector Boson in the $qqbb$ Final State with the ATLAS Detector

G. Aad *et al.*\*  
(ATLAS Collaboration)

 (Received 14 December 2023; accepted 26 February 2024; published 28 March 2024)

This Letter presents the first study of Higgs boson production in association with a vector boson ( $V = W$  or  $Z$ ) in the fully hadronic  $qqbb$  final state using data recorded by the ATLAS detector at the LHC in proton-proton collisions at  $\sqrt{s} = 13$  TeV and corresponding to an integrated luminosity of  $137 \text{ fb}^{-1}$ . The vector bosons and Higgs bosons are each reconstructed as large-radius jets and tagged using jet substructure techniques. Dedicated tagging algorithms exploiting  $b$ -tagging properties are used to identify jets consistent with Higgs bosons decaying into  $b\bar{b}$ . Dominant backgrounds from multijet production are determined directly from the data, and a likelihood fit to the jet mass distribution of Higgs boson candidates is used to extract the number of signal events. The  $VH$  production cross section is measured inclusively and differentially in several ranges of Higgs boson transverse momentum: 250–450, 450–650, and greater than 650 GeV. The inclusive signal yield relative to the standard model expectation is observed to be  $\mu = 1.4_{-0.9}^{+1.0}$  and the corresponding cross section is  $3.1 \pm 1.3(\text{stat})_{-1.4}^{+1.8}(\text{syst}) \text{ pb}$ .

DOI: [10.1103/PhysRevLett.132.131802](https://doi.org/10.1103/PhysRevLett.132.131802)

In the standard model (SM) of particle physics, the Brout-Englert-Higgs mechanism [1–4] spontaneously breaks electroweak symmetry. As a result, a physical Higgs boson emerges and both the  $W$  and  $Z$  gauge bosons and the fermions acquire mass. Since the discovery of the Higgs boson by the ATLAS and CMS experiments at the LHC [5,6], precision measurements of its properties have been a priority for both experiments. The Higgs boson decay into bottom-quark pairs ( $H \rightarrow b\bar{b}$ ) has the largest branching fraction ( $\sim 58\%$ ) [7] and has only recently been observed by exploiting associated production with a vector boson ( $VH$ ,  $V = W, Z$ ) [8,9]. In these analyses, the associated  $W$  and  $Z$  bosons were required to decay leptonically to provide both a means to trigger these events and an effective suppression of the large background from QCD production of  $b$  quarks. Theoretical work has raised interest in testing for new physics contributions to associated  $VH$  production at high momentum by exploiting  $H \rightarrow b\bar{b}$  decays in a highly boosted event topology [10–12] because of its sensitivity to higher-order effective operators. On the experimental side, ATLAS and CMS have successfully developed and calibrated novel jet-substructure techniques to identify high-momentum  $V$  or  $H$  bosons that decay hadronically and are reconstructed as a single large-radius

(“large- $R$ ”) jet. Dedicated tagging algorithms exploiting  $b$ -tagging properties are used to identify jets consistent with Higgs bosons decaying into  $b\bar{b}$ .

In this Letter, these experimental techniques are applied in a first study of associated  $VH$  production at high Higgs boson transverse momentum ( $p_T^H$ ) in the two large- $R$  jets topology. This approach has the potential to probe higher  $p_T^H$  values than in the best current measurement in the semileptonic final state [13] because the  $W/Z$  hadronic branching fractions are larger. The  $VH$  signal is extracted using a likelihood fit to the invariant mass distribution of Higgs candidate large- $R$  jets in events also containing a  $W$ - or  $Z$ -candidate jet. The dominant multijet background is estimated directly from the data, while smaller backgrounds ( $t\bar{t}$ ,  $V$  + jets, and  $VV$  production) are modeled using Monte Carlo (MC) simulation. The normalization of the peaking  $Z$  + jets background (mostly from  $Z \rightarrow b\bar{b}$  decays passing as Higgs candidates) is a free parameter in the final fit. The selected events are separated into several  $p_T^H$  ranges and the  $VH$  production cross section is measured both inclusively and as a function of  $p_T^H$ .

The analysis presented here uses the proton-proton collision data collected by the ATLAS detector [14–16] from 2015 to 2018, corresponding to an integrated luminosity of  $137 \text{ fb}^{-1}$  at  $\sqrt{s} = 13$  TeV. The ATLAS detector is a multipurpose particle detector with cylindrical geometry. It consists of an inner tracking detector surrounded by a superconducting solenoid, sampling electromagnetic and hadronic calorimeters, and a muon spectrometer with three toroidal superconducting magnets, providing a near  $4\pi$  coverage in solid angle [17]. A two-level trigger

\*Full author list given at the end of the Letter.

Published by the American Physical Society under the terms of the [Creative Commons Attribution 4.0 International license](https://creativecommons.org/licenses/by/4.0/). Further distribution of this work must maintain attribution to the author(s) and the published article's title, journal citation, and DOI. Funded by SCOAP<sup>3</sup>.

system [18] selects events for storage. An extensive software suite [19] is used in data simulation, in the reconstruction and analysis of real and simulated data, in detector operations, and in the trigger and data acquisition systems of the experiment. Collision events satisfy a number of requirements ensuring that the ATLAS detector was operating well while the data were recorded.

Simulated events were produced for a variety of processes. All generated events were passed through a full simulation of the ATLAS detector response [20] using GEANT4 [21]. The effects of multiple  $pp$  interactions in the same or neighboring bunch crossings (pileup) were included by overlaying events generated with PYTHIA8 [22]. Events were weighted such that the distribution of the average number of interactions per bunch crossing matches that observed in data.

Higgs boson events were generated at next-to-leading-order (NLO) accuracy via gluon-gluon fusion, vector-boson fusion, and in association with a vector boson ( $VH$ ) using POWHEG BOX v2 [23–26] and the PDF4LHC15NLO parton distribution function (PDF) set [27]. The loop-induced  $gg \rightarrow ZH$  process was generated separately at leading order (LO) with POWHEG BOX. In these cases, the events were interfaced with PYTHIA8 [22] utilizing the AZNLO tune [28] to incorporate parton shower and nonperturbative effects. The production of a Higgs boson in association with two top quarks ( $t\bar{t}H$ ) was modeled similarly, using POWHEG BOX v2 with the NNPDF3.0NLO PDF set [29] and the A14 tune [30]. Other Higgs boson production mechanisms such as  $tH$  and QCD-induced  $b\bar{b}H$  are not considered since their contribution is negligible. The simulated processes are normalized using the best available cross-section calculations [7]. In particular, the  $pp \rightarrow VH$  cross section is calculated to next-to-next-to-leading order in QCD with NLO electroweak (EW) corrections, and the  $gg \rightarrow ZH$  cross section is calculated at NLO and next-to-leading-logarithm accuracy [31–37]. The  $q\bar{q}/qg \rightarrow ZH$  simulated events are normalized using the  $pp \rightarrow ZH$  cross section (which combines the  $q\bar{q}$ ,  $qg$ , and  $gg$  contributions) after subtracting the  $gg \rightarrow ZH$  cross section. Differential NLO EW corrections computed with HAWK [35] are applied to the  $q\bar{q}/qg \rightarrow VH$  process as a function of vector-boson transverse momentum,  $p_T^V$ .

Simulated multijet events are only used to optimize the event selection since the multijet background is estimated directly from the data, as described later. They were generated using PYTHIA8 with LO matrix elements for dijet production. The NNPDF2.3LO PDF set [38] and A14 tune were used in all steps of the event generation. Samples of  $V + \text{jets}$  events were generated with SHERPA2.2.8 [39] and the NNPDF3.0NLO PDF set at NLO accuracy for one additional parton and LO accuracy for up to four additional partons. All generated  $V + \text{jets}$  samples have NLO QCD and LO EW accuracy. Additional NLO EW corrections are applied to the simulated events as weights. Diboson events

( $VV = WW, WZ, ZZ$ ) were generated with SHERPA2.2.8 and the NNPDF3.0NLO PDF set at NLO accuracy for up to one additional parton and LO accuracy for up to three additional partons. The simulated  $t\bar{t}$  events were generated at NLO using POWHEG BOX v2 with  $h_{\text{damp}} = 1.5m_{\text{top}}$  [40]. Weights are also applied to match the  $t\bar{t}$  yields measured in data in the same kinematic phase space [41]. Single-top production in the  $Wt$  channel was modeled at NLO using POWHEG BOX v2 in the five-flavor scheme [42] and with the diagram removal scheme [40] to treat interference with  $t\bar{t}$  production. The NNPDF3.0NLO PDF set was used for all top-quark samples. Except for Sherpa samples, the decay of  $b$  and  $c$  hadrons was performed using EvtGen1.6.0 [43].

Events are required to pass single large- $R$  jet triggers [18], with mass and transverse momentum exceeding specific thresholds. The event selection described below is designed to ensure full trigger efficiency. Events are also required to have a primary vertex with at least two associated tracks. The primary vertex is selected as the vertex with the largest  $\Sigma p_T^2$ , where the sum is over all of its associated tracks with  $p_T > 0.5$  GeV [44]. In addition, noncollision backgrounds originating from calorimeter noise, beam halo interactions or cosmic rays are suppressed by rejecting events that contain any anti- $k_t$  calorimeter jet with  $R = 0.4$  failing to satisfy a set of quality criteria [45].

Large- $R$  jets are used to identify both the  $V$  boson and the Higgs boson. They are reconstructed with the anti- $k_t$  algorithm [46,47] with a radius parameter of  $R = 1.0$ , utilizing locally weighted topological cell clusters [48] for their constituents. At this stage, these jets are referred to as ungroomed jets. Jets are then trimmed [49] to remove energy deposits from pileup and the underlying event as well as soft and wide-angle radiation. The jet mass is reconstructed by combining the calorimeter and tracking measurements [50], where tracks are required to be associated with the primary vertex.

To aid in  $H \rightarrow b\bar{b}$  tagging of large- $R$  jets, a separate collection of jets is built from tracks with the anti- $k_t$  algorithm using a  $p_T$ -dependent radius [51]. Variable-radius track jets are then matched to large- $R$  calorimeter jets via ghost association [52] and used as proxies for  $b$  quarks associated with the Higgs candidate. All large- $R$  jets must satisfy  $p_T > 200$  GeV and  $|\eta| < 2.0$  to ensure they are contained within the tracking detector. Events with one or more isolated charged leptons (electrons or muons) are rejected. Electrons are identified by matching tracks to energy clusters in the electromagnetic calorimeter. They must have  $p_T > 7$  GeV and  $|\eta| < 2.5$ , and satisfy the “loose” identification criterion defined in Ref. [53]. Muon identification relies on matching tracks in the inner detector to muon spectrometer tracks or track segments. Muons must have  $p_T > 7$  GeV and  $|\eta| < 2.5$ , and satisfy the loose selection criterion [54].

The identification of  $W$  and  $Z$  bosons relies on several properties of the large- $R$  jets. The  $D_2^{\beta=1}$  variable exploits the two-prong structure of the  $W/Z \rightarrow qq$  decays, absent in typical QCD jets [55,56]. The number of tracks ( $N_{\text{trk}}$ ) linked to the ungroomed large- $R$  jets by ghost association is significantly higher for gluon-induced jets in background events than for quark-induced jets in signal events, due to the distinct energy scales involved and the different color factors for gluons and quarks. Requirements on the jet mass,  $D_2^{\beta=1}$ , and  $N_{\text{trk}}$  are optimized as a function of jet  $p_T$  such that a signal efficiency of 50% [57] is achieved in each jet- $p_T$  category, along with a multijet background rejection factor of 70–200. The  $W$  boson tagging is calibrated with semileptonic  $t\bar{t}$  data events and then extrapolated to the identification of  $Z$  bosons [57]. For the high- $p_T$  category, an additional uncertainty is applied to the  $Z$ -boson tagging, based on differences between  $W$ -boson to  $Z$ -boson tagging efficiency extrapolations obtained with SHERPA and HERWIG.

Higgs candidates are identified by an  $H \rightarrow b\bar{b}$  tagger [58] based on a neural-network algorithm that uses track and vertex information from the variable-radius track jets to discriminate between large- $R$  jets from Higgs boson decays into  $b\bar{b}$  and jets from gluons, light quarks, or top quarks. A fixed 60% signal efficiency working point (WP) is used, where 60% refers to the average efficiency for selecting simulated Higgs bosons with  $p_T > 250$  GeV [58]. The jet mass resolution for Higgs candidates is improved by applying a “muon-in-jet” correction to account for the energy carried by muons from semileptonic  $b$ -hadron decays [59]. The corrected jet mass of the Higgs boson candidate ( $m_J^H$ ) is used to extract the signal.

Events are required to contain at least two selected large- $R$  jets. The leading (highest  $p_T$ ) large- $R$  jet must have  $p_T > 450$  GeV and mass above 50 GeV, to ensure full trigger efficiency. The second leading large- $R$  jet must have a mass above 40 GeV. At least one of those two jets must pass the  $H \rightarrow b\bar{b}$  tagger requirements. If both jets satisfy those requirements, the one with a larger mass is selected as the Higgs candidate. The other jet must then satisfy the  $W/Z$  tagging requirements. Furthermore, the Higgs candidate’s transverse momentum ( $p_{T,J}^H$ ) must exceed 250 GeV, thereby defining the signal region (SR), and three exclusive ranges are chosen:  $p_{T,J}^H \in [250, 450)$  GeV,  $p_{T,J}^H \in [450, 650)$  GeV, and  $p_{T,J}^H \geq 650$  GeV. In the SR, the  $VH$  process dominates (85%), although other Higgs boson production processes contribute:  $t\bar{t}H$  (8%), gluon-gluon fusion (6%), and vector-boson fusion (1.4%). The dominant background contribution comes from multijet production (90%), followed by  $t\bar{t}$  (5%),  $V + \text{jets}$  (3.6%), and diboson (0.7%) production. A data-driven method is used to estimate the background contribution from multijet production as well as that from  $V + \text{jets}$  production in which the  $W/Z$  boson is correctly tagged and the additional jet is a QCD jet misidentified as

the Higgs candidate (both processes are referred to as “multijet”). Other background processes are modeled by simulation, including  $V + \text{jets}$  production in which the  $W/Z$  boson is selected as the Higgs candidate and a QCD jet passes the  $V$  tagging requirements.

The multijet background estimate is extracted from a control region (CR) where events pass all SR requirements except the Higgs tagging requirement, since the  $H \rightarrow b\bar{b}$  tagger does not rely on the jet mass as a discriminating variable. To account for differences in distribution shape and normalization between the SR and CR, a transfer factor (TF), which depends on both jet  $p_T$  and jet mass ( $m$ ), is used. The number of multijet events in the SR is thus derived from the number of multijet events in the CR ( $N_{\text{multijet}}^{\text{CR}}$ ) as

$$N_{\text{multijet}}^{\text{SR}}(p_T, m) = \text{TF}(p_T, \rho) \times N_{\text{multijet}}^{\text{CR}}(p_T, m),$$

where  $\text{TF}(p_T, \rho) = \sum_{k,l} \alpha_{kl} \rho^k p_T^l$ ,  $\rho = \log(m^2/p_T^2)$ , and  $\alpha_{kl}$  are the polynomial coefficients for the  $k$ th order in  $\rho$  and  $l$ th order in  $p_T$ . The  $\alpha_{kl}$  coefficients are determined from a simultaneous fit to the data in the SR and CR across the whole jet mass range. To determine the order of the polynomial needed to fit the data, a Fisher  $F$  test is performed. Based on its results, a first-order polynomial in both  $\rho$  and  $p_T$  is found to be sufficient to parametrize the transfer factor in the SR.

Three validation regions were defined to verify that the multijet background estimated using the TF method describes the observed background well. Events in these regions contain a  $V$  jet passing the looser  $W/Z$  tagging 80% efficiency WP [57] but failing either the  $N_{\text{trk}}$ ,  $D_2^{\beta=1}$ , or mass requirement corresponding to the nominal 50% efficiency WP. The composition of events from background processes in these regions, as tested with simulated samples, is similar to that in the SR. The background modeling is found to be in good agreement with data within the statistical uncertainty in each of the validation regions.

A second multijet background estimation method is utilized to test the nominal TF method. A boosted decision tree (BDT), trained on an alternative set of data events that fail both the  $V$  and Higgs boson tagging, is used to perform a kinematic reweighting to match the kinematic distributions in this alternative region to those in the SR. A description of this reweighting procedure is available in Ref. [60]. The two multijet background estimates agree within statistical uncertainties.

Systematic uncertainties arise from several different sources: the data-driven background estimate, the experimental reconstruction, and the theoretical prediction for the signal. Their impact is summarized in the Appendix. The uncertainty affecting the shape of the estimated multijet background is evaluated as the difference between the distributions from the BDT and TF methods. It is found to

be up to 10% for  $p_{T,J}^H \in [250, 650)$  GeV and up to 20% for  $p_{T,J}^H$  above 650 GeV.

Uncertainties in the modeling of the subdominant  $VV$  and  $t\bar{t}$  backgrounds include normalization uncertainties of 80% [13] and 12% [61], respectively, as well as changes in the shape of the  $m_J^H$  distribution when using different renormalization and factorization scales or alternative event generators. The effect of scale uncertainties on the  $m_J^H$  distribution's shape is also included for the  $Z + \text{jets}$  background. Uncertainties in the modeling of the  $Wt$  background have negligible impact.

Experimental uncertainties related to large- $R$  jets,  $W/Z$  tagging, and  $H \rightarrow b\bar{b}$  tagging affect the predicted event yields for the signal and the  $VV$ ,  $V + \text{jets}$ , and  $t\bar{t}$  backgrounds. Uncertainties in the scale and resolution of the large- $R$  jet energy and mass measurements affect the shape of the  $m_J^H$  distribution and are evaluated following Ref. [50].

Uncertainties in the  $W/Z$  tagging are determined from studies of  $t\bar{t}$  events in data [57,62]. The  $H \rightarrow b\bar{b}$  tagging efficiency is measured in a sample enriched in  $Z \rightarrow b\bar{b}$  decays [63]. The resulting scale factors are applied to the simulation and vary between 0.86 and 1.80 across the  $p_T$  bins, with uncertainties in the range 30%–60%. These scale factors are further constrained in the fit to data by the presence of the  $W/Z$  resonances in the jet mass distribution.

The impact of uncertainties in the PDF sets, initial- and final-state radiation, and multiparton interactions on the signal acceptance is included. Uncertainties related to the PDF sets are derived by applying the methodology outlined by the PDF4LHC group [27] and considering four additional PDF sets (CT14, MMHT2014, NNPDF3.0, and ATLAS-epWZ12), resulting in 3% uncertainties in the signal acceptance. An uncertainty of 0.83% is applied to the integrated luminosity [64].

The signal yield and the  $Z + \text{jets}$  normalization are extracted from a simultaneous binned maximum-likelihood fit to the  $m_J^H$  distributions in the SR (shown in Fig. 1) and CR in the range 60–200 GeV. Confidence intervals are based on the profile-likelihood-ratio test statistic [65,66]. Systematic uncertainties are implemented in the fit as nuisance parameters constrained by Gaussian or log-normal likelihood terms, and the Higgs boson mass is assumed to be  $m_H = 125.09 \pm 0.24$  GeV. The overall normalization factor for the peaking component of the  $Z + \text{jets}$  background (mostly from  $Z \rightarrow b\bar{b}$  decays) from the fit is  $1.4_{-0.6}^{+0.8}$ .

The best-fit value of the signal-strength parameter, defined as the ratio of the observed signal yield to that expected in the SM, is  $\mu = 1.4_{-0.9}^{+1.0}$  for the inclusive fit, corresponding to an observed (expected) significance of  $1.7\sigma$  ( $1.2\sigma$ ) with respect to the null signal hypothesis. An inclusive cross section of 2.24 pb [67] is used to normalize the expected signal. The statistical uncertainty in  $\mu$  is 0.6, whereas the systematic uncertainty is  $_{-0.6}^{+0.8}$ .

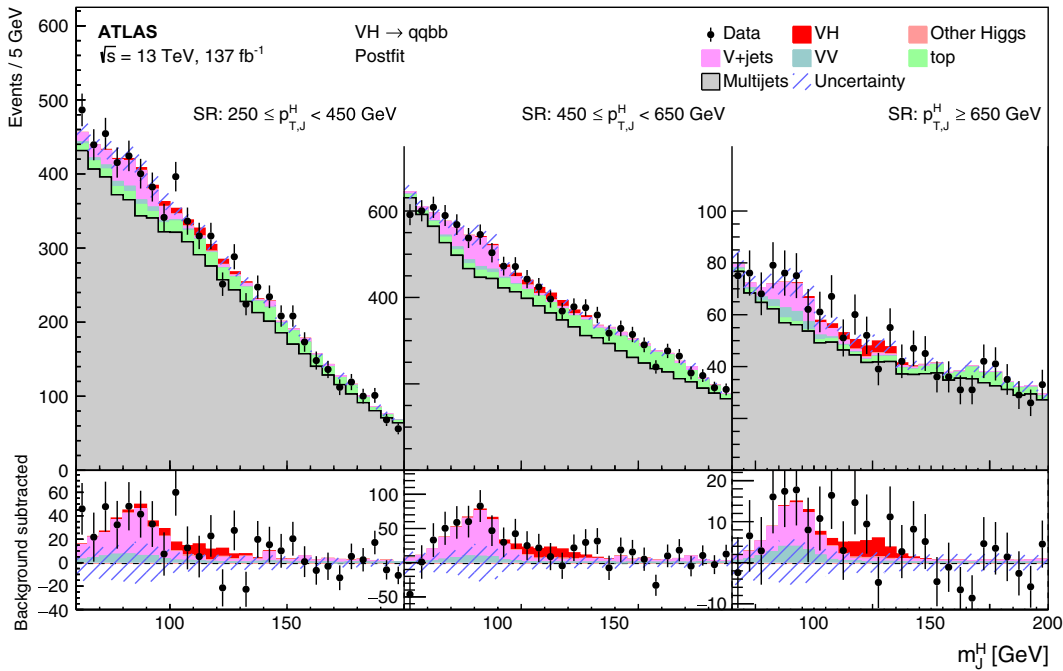


FIG. 1. Higgs candidate jet mass distributions in the signal region for  $p_{T,J}^H \in [250, 450)$  GeV (left),  $p_{T,J}^H \in [450, 650)$  GeV (middle), and  $p_{T,J}^H \geq 650$  GeV (right) obtained after the inclusive fit with a single  $Z + \text{jets}$  normalization factor and a single signal strength. The bottom panels show the distributions after subtracting the multijet and top-quark backgrounds. The hatched bands show the total uncertainty in the background estimate.

TABLE I. Signal strengths ( $\mu$ ) and cross sections ( $\sigma$ ) in exclusive kinematic regions. The expected cross sections are based on the inclusive cross section from Ref. [67] and the acceptance values derived from the signal simulation. The upper limits on the cross section provided in parentheses are quoted at the 95% confidence level.

Kinematic region	Observed $\mu$	Observed $\sigma$ [fb]	Expected $\sigma$ [fb]
$250 \leq p_T^H < 450$ GeV, $ y_H  < 2$	$0.8^{+2.2}_{-1.9}$	$47^{+125}_{-109}$ ( $< 363$ )	57.0
$450 \leq p_T^H < 650$ GeV, $ y_H  < 2$	$0.4^{+1.7}_{-1.5}$	$2^{+10}_{-9}$ ( $< 24$ )	5.9
$p_T^H \geq 650$ GeV, $ y_H  < 2$	$5.3^{+11.3}_{-3.2}$	$6^{+13}_{-4}$ ( $< 43$ )	1.2

The latter is dominated by the shape of the estimated multijet background and the  $H \rightarrow b\bar{b}$  tagging scale factors. The corresponding inclusive cross section is  $3.1 \pm 1.3(\text{stat})^{+1.8}_{-1.4}(\text{syst})$  pb.

The signal strengths and cross sections are also extracted in three exclusive kinematic regions defined at generator level by  $p_T^H \in [250, 450)$  GeV,  $p_T^H \in [450, 650)$  GeV, and  $p_T^H \geq 650$  GeV, with  $|y_H| < 2$  required in each region. The results are obtained using  $m_J^H$  templates extracted from the signal MC samples with the kinematic requirements applied for each region. Those results are presented in Table I.

In conclusion, a first study of associated  $VH$  production is performed in the fully hadronic final state, reaching Higgs boson transverse momenta at the TeV scale. A likelihood fit to the mass distribution of Higgs candidate large- $R$  jets in events also containing a  $W$  or  $Z$  candidate jet is used to extract the  $VH$  signal both inclusively and as a function of transverse momentum. The significance of the  $VH$  signal is estimated to be  $1.7\sigma$  and the inclusive cross section is determined to be  $3.1 \pm 1.3(\text{stat})^{+1.8}_{-1.4}(\text{syst})$  pb, in agreement with the SM prediction. While the current study is limited by large uncertainties, this channel will open a kinematic region with high sensitivity to new physics contributions when larger data samples are collected.

We thank CERN for the very successful operation of the LHC, as well as the support staff from our institutions without whom ATLAS could not be operated efficiently. We acknowledge the support of ANPCyT, Argentina; YerPhI, Armenia; ARC, Australia; BMWFW and FWF, Austria; ANAS, Azerbaijan; CNPq and FAPESP, Brazil; NSERC, NRC, and CFI, Canada; CERN; ANID, Chile; CAS, MOST, and NSFC, China; Minciencias, Colombia; MEYS CR, Czech Republic; DNRF and DNSRC, Denmark; IN2P3-CNRS and CEA-DRF/IRFU, France; SRNSFG, Georgia; BMBF, HGF, and MPG, Germany; GSRI, Greece; RGC and Hong Kong SAR, China; ISF and Benozio Center, Israel; INFN, Italy; MEXT and JSPS, Japan; CNRST, Morocco; NWO, Netherlands; RCN, Norway; MEiN, Poland; FCT, Portugal; MNE/IFA, Romania; MESTD, Serbia; MSSR, Slovakia; ARRS and MIZŠ, Slovenia; DSI/NRF, South Africa; MICINN, Spain; SRC and Wallenberg Foundation, Sweden; SERI, SNSF, and Cantons of Bern and Geneva, Switzerland; MOST,

Taipei; TENMAK, Türkiye; STFC, United Kingdom; DOE and NSF, USA. In addition, individual groups and members have received support from BCKDF, CANARIE, CRC, and DRAC, Canada; PRIMUS 21/SCI/017 and UNCE SCI/013, Czech Republic; COST, ERC, ERDF, Horizon 2020, ICSC-NextGenerationEU, and Marie Skłodowska-Curie Actions, European Union; Investissements d’Avenir Labex, Investissements d’Avenir IDEX, and ANR, France; DFG and AvH Foundation, Germany; Herakleitos, Thales, and Aristeia programmes co-financed by EU-ESF and the Greek NSRF, Greece; BSF-NSF and MINERVA, Israel; Norwegian Financial Mechanism 2014-2021, Norway; NCN and NAWA, Poland; La Caixa Banking Foundation, CERCA Programme Generalitat de Catalunya and PROMETEO and GenT Programmes Generalitat Valenciana, Spain; Göran Gustafssons Stiftelse, Sweden; The Royal Society and Leverhulme Trust, United Kingdom. The crucial computing support from all WLCG partners is acknowledged gratefully, in particular from CERN, the ATLAS Tier-1 facilities at TRIUMF/SFU (Canada), NDGF (Denmark, Norway, Sweden), CC-IN2P3 (France), KIT/GridKA (Germany), INFN-CNAF (Italy), NL-T1 (Netherlands), PIC (Spain), RAL (UK), and BNL (USA), the Tier-2 facilities worldwide and large non-WLCG resource providers. Major contributors of computing resources are listed in Ref. [68].

*Appendix.*—The Monte Carlo simulation does not provide an accurate description of the QCD multijet background, especially in the high- $p_T$  kinematic region, motivating the need for a dedicated estimate of the multijet contribution in the phase space selected for this study. Therefore, this analysis exploits a fully data-driven estimation of the multijet background, using events in both the signal and control regions while testing it in validation regions. Two different methods are compared for the data-driven estimation. First, the transfer factor (TF) method uses a jet  $p_T$ - and mass-dependent transfer function to predict the yields of events that pass the event selection from the events that fail the Higgs boson tagging. The multijet background estimation and the signal extraction are performed simultaneously. Second, the boosted decision tree (BDT) method extracts the background templates from the events failing the  $V$  and Higgs boson tagging. A BDT is

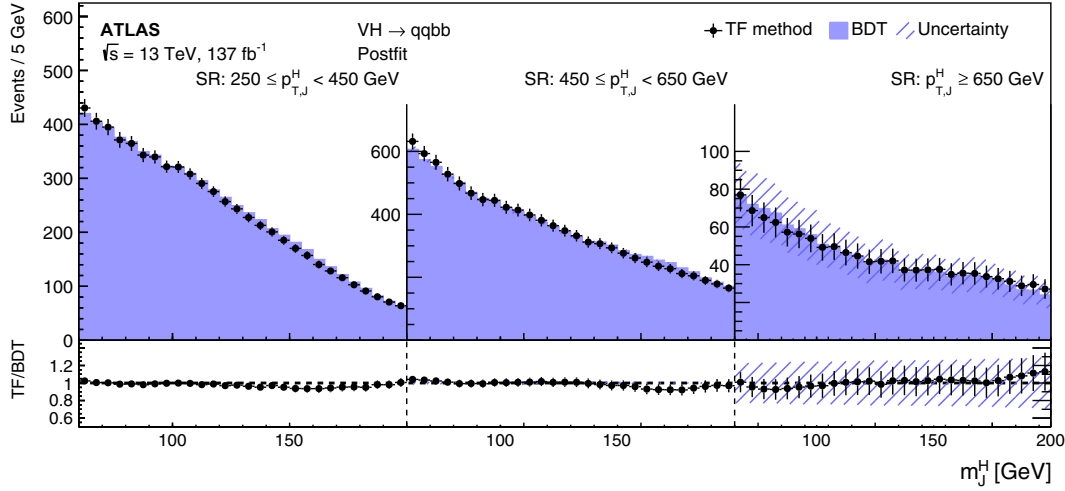


FIG. 2. Higgs candidate jet mass distributions for the multijet background in the signal region estimated with either the nominal transfer factor method (TF) or the boosted decision tree method (BDT). The error bars (hatched uncertainty band) represent(s) the total uncertainty in the TF (BDT) estimate including both the statistical and systematic uncertainties. The BDT uncertainties comprise a statistical component obtained using the method from Ref. [60] and the difference between the data and the background estimate in the validation regions. This difference is relatively large in the last  $p_T$  bin. It should be noted that there is a strong statistical correlation between the distributions from the two methods and that the BDT uncertainties are small in the first two  $p_T$  bins.

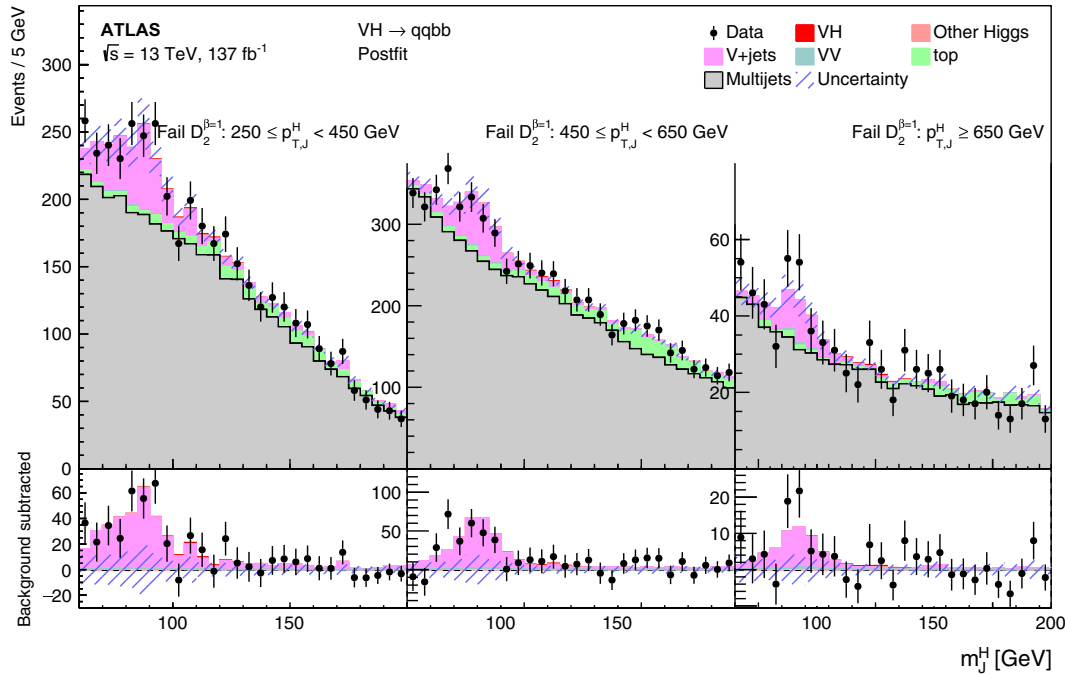


FIG. 3. Higgs candidate jet mass distributions after the inclusive fit in the validation region consisting of events passing the 80% efficiency working point of the  $V$ -jet tagger but failing only the  $D_2^{\beta=1}$  requirement of its tighter 50% efficiency working point. No  $H \rightarrow b\bar{b}$  tagging is applied. The bottom panels show the distributions after subtracting the multijet and top-quark backgrounds. The hatched bands show the total uncertainty in the background estimate.

used to perform a kinematic reweighting by predicting the event weights needed to bring the shapes of kinematic distributions in the control and signal regions into agreement. The following variables are used in the BDT training: Higgs candidate large- $R$  jet  $p_T$ , mass,

pseudorapidity, and azimuthal angle, as well as the number of associated tracks and track jets.

The two methods give consistent results. After studying the fit to the sidebands and the uncertainties in the signal-plus-background Asimov fit [66] to the signal region, the

TABLE II. Breakdown of the various sources of uncertainty in the inclusive signal strength  $\mu$ .

Uncertainty source	$\delta\mu$
Signal modeling	+0.10 -0.02
MC statistical uncertainty	+0.13 -0.13
Instrumental (pileup, luminosity)	+0.012 -0.004
Large- $R$ jet	+0.13 -0.14
Top-quark modeling	+0.14 -0.15
Other theory modeling	+0.05 -0.03
$H \rightarrow b\bar{b}$ tagging	+0.52 -0.23
Multijet estimate (TF uncertainty)	+0.52 -0.41
Multijet modeling (TF vs BDT)	+0.14 -0.18
Total systematic uncertainty	+0.80 -0.61
Signal statistical uncertainty	+0.60 -0.60
Z + jets normalization	+0.42 -0.20
Total statistical uncertainty	+0.63 -0.63
Total uncertainty	+1.02 -0.88

TF method was selected as the background estimation method, while the BDT method provides a robust and important cross-check of the results obtained and is used as an alternative method to determine shape systematic uncertainties. A comparison of the Higgs candidate jet mass distributions for the multijet background estimates from the two methods is shown in Fig. 2.

As another test of the background estimation, the statistical analysis is applied to the validation and control regions. Figure 3 presents the Higgs candidate jet mass distributions in one of the validation regions and demonstrates good agreement between the data and the background model.

The impact of the different sources of uncertainty on the signal strength is presented in Table II.

[1] F. Englert and R. Brout, Broken symmetry and the mass of gauge vector mesons, *Phys. Rev. Lett.* **13**, 321 (1964).  
 [2] P. W. Higgs, Broken symmetries and the masses of gauge bosons, *Phys. Rev. Lett.* **13**, 508 (1964).  
 [3] P. W. Higgs, Broken symmetries, massless particles and gauge fields, *Phys. Lett.* **12**, 132 (1964).  
 [4] G. S. Guralnik, C. R. Hagen, and T. W. B. Kibble, Global conservation laws and massless particles, *Phys. Rev. Lett.* **13**, 585 (1964).  
 [5] ATLAS Collaboration, Observation of a new particle in the search for the Standard Model Higgs boson with the ATLAS detector at the LHC, *Phys. Lett. B* **716**, 1 (2012).  
 [6] CMS Collaboration, Observation of a new boson at a mass of 125 GeV with the CMS experiment at the LHC, *Phys. Lett. B* **716**, 30 (2012).

[7] D. de Florian *et al.*, Handbook of LHC Higgs cross sections: 4. Deciphering the nature of the Higgs Sector, [arXiv:1610.07922](https://arxiv.org/abs/1610.07922).  
 [8] ATLAS Collaboration, Observation of  $H \rightarrow b\bar{b}$  decays and  $VH$  production with the ATLAS detector, *Phys. Lett. B* **786**, 59 (2018).  
 [9] CMS Collaboration, Observation of Higgs boson decay to bottom quarks, *Phys. Rev. Lett.* **121**, 121801 (2018).  
 [10] J. Brehmer, S. Dawson, S. Homiller, F. Kling, and T. Plehn, Benchmarking simplified template cross sections in  $WH$  production, *J. High Energy Phys.* **11** (2019) 034.  
 [11] A. Biekötter, A. Knochel, M. Krämer, D. Liu, and F. Riva, Vices and virtues of Higgs effective field theories at large energy, *Phys. Rev. D* **91**, 055029 (2015).  
 [12] K. Mimasu, V. Sanz, and C. Williams, Higher Order QCD predictions for associated Higgs production with anomalous couplings to gauge bosons, *J. High Energy Phys.* **08** (2016) 039.  
 [13] ATLAS Collaboration, Measurement of the associated production of a Higgs boson decaying into  $b$ -quarks with a vector boson at high transverse momentum in  $pp$  collisions at  $\sqrt{s} = 13$  TeV with the ATLAS detector, *Phys. Lett. B* **816**, 136204 (2021).  
 [14] ATLAS Collaboration, The ATLAS experiment at the CERN Large Hadron Collider, *J. Instrum.* **3**, S08003 (2008).  
 [15] ATLAS Collaboration, ATLAS Insertable B-Layer: Technical Design Report No. ATLAS-TDR-19; CERN-LHCC-2010-013, 2010, <https://cds.cern.ch/record/1291633>; Addendum: Report No. ATLAS-TDR-19-ADD-1; CERN-LHCC-2012-009, 2012, <https://cds.cern.ch/record/1451888>.  
 [16] B. Abbott *et al.*, Production and integration of the ATLAS insertable B-layer, *J. Instrum.* **13**, T05008 (2018).  
 [17] ATLAS uses a right-handed coordinate system with its origin at the nominal interaction point in the center of the detector and the  $z$  axis along the beam pipe. The  $x$  axis points to the center of the LHC ring, and the  $y$  axis points upward. Cylindrical coordinates  $(r, \phi)$  are used in the transverse plane,  $\phi$  being the azimuthal angle around the  $z$  axis. The pseudorapidity is defined in terms of the polar angle  $\theta$  as  $\eta = -\ln \tan(\theta/2)$ . Angular distance is measured in units of  $\Delta R \equiv \sqrt{(\Delta\eta)^2 + (\Delta\phi)^2}$ .  
 [18] ATLAS Collaboration, Performance of the ATLAS trigger system in 2015, *Eur. Phys. J. C* **77**, 317 (2017).  
 [19] ATLAS Collaboration, The ATLAS Collaboration Software and Firmware, Report No. ATL-SOFT-PUB-2021-001, 2021, <https://cds.cern.ch/record/2767187>.  
 [20] ATLAS Collaboration, The ATLAS simulation Infrastructure, *Eur. Phys. J. C* **70**, 823 (2010).  
 [21] S. Agostinelli *et al.*, GEANT4—a simulation toolkit, *Nucl. Instrum. Methods Phys. Res., Sect. A* **506**, 250 (2003).  
 [22] T. Sjöstrand, S. Ask, J. R. Christiansen, R. Corke, N. Desai, P. Ilten, S. Mrenna, S. Prestel, C. O. Rasmussen, and P. Z. Skands, An introduction to PYTHIA8.2, *Comput. Phys. Commun.* **191**, 159 (2015).  
 [23] P. Nason and C. Oleari, NLO Higgs boson production via vector-boson fusion matched with shower in POWHEG, *J. High Energy Phys.* **02** (2010) 037.  
 [24] S. Alioli, P. Nason, C. Oleari, and E. Re, A general framework for implementing NLO calculations in shower

- Monte Carlo programs: the POWHEG BOX, *J. High Energy Phys.* **06** (2010) 043.
- [25] P. Nason, A new method for combining NLO QCD with shower Monte Carlo algorithms, *J. High Energy Phys.* **11** (2004) 040.
- [26] S. Frixione, P. Nason, and C. Oleari, Matching NLO QCD computations with parton shower simulations: The POWHEG method, *J. High Energy Phys.* **11** (2007) 070.
- [27] J. Butterworth *et al.*, PDF4LHC recommendations for LHC Run II, *J. Phys. G* **43**, 023001 (2016).
- [28] ATLAS Collaboration, Measurement of the  $Z/\gamma^*$  boson transverse momentum distribution in  $pp$  collisions at  $\sqrt{s} = 7$  TeV with the ATLAS detector, *J. High Energy Phys.* **09** (2014) 145.
- [29] R. D. Ball *et al.* (NNPDF Collaboration), Parton distributions for the LHC run II, *J. High Energy Phys.* **04** (2015) 040.
- [30] ATLAS Collaboration, ATLAS PYTHIA8 tunes to 7 TeV data, ATL-PHYS-PUB-2014-021, 2014, <https://cds.cern.ch/record/1966419>.
- [31] M. L. Ciccolini, S. Dittmaier, and M. Krämer, Electroweak radiative corrections to associated  $WH$  and  $ZH$  production at hadron colliders, *Phys. Rev. D* **68**, 073003 (2003).
- [32] O. Brein, A. Djouadi, and R. Harlander, NNLO QCD corrections to the Higgs-strahlung processes at hadron colliders, *Phys. Lett. B* **579**, 149 (2004).
- [33] O. Brein, R. V. Harlander, M. Wiesemann, and T. Zirke, Top-quark mediated effects in hadronic Higgs-Strahlung, *Eur. Phys. J. C* **72**, 1868 (2012).
- [34] L. Altenkamp, S. Dittmaier, R. V. Harlander, H. Rzehak, and T. J. E. Zirke, Gluon-induced Higgs-strahlung at next-to-leading order QCD, *J. High Energy Phys.* **02** (2013) 078.
- [35] A. Denner, S. Dittmaier, S. Kallweit, and A. Mück, HAWK2.0: A Monte Carlo program for Higgs production in vector-boson fusion and Higgs strahlung at hadron colliders, *Comput. Phys. Commun.* **195**, 161 (2015).
- [36] O. Brein, R. V. Harlander, and T. J. E. Zirke, `vh@nnlo`—Higgs Strahlung at hadron colliders, *Comput. Phys. Commun.* **184**, 998 (2013).
- [37] R. V. Harlander, A. Kulesza, V. Theeuwes, and T. Zirke, Soft gluon resummation for gluon-induced Higgs Strahlung, *J. High Energy Phys.* **11** (2014) 082.
- [38] R. D. Ball *et al.* (NNPDF Collaboration), Parton distributions with LHC data, *Nucl. Phys.* **B867**, 244 (2013).
- [39] T. Gleisberg, S. Höche, F. Krauss, M. Schönherr, S. Schumann, F. Siegert, and J. Winter, Event generation with SHERPA1.1, *J. High Energy Phys.* **02** (2009) 007.
- [40] ATLAS Collaboration, Studies on top-quark Monte Carlo modelling for Top2016, Report No. ATL-PHYS-PUB-2016-020, 2016, <https://cds.cern.ch/record/2216168>.
- [41] ATLAS Collaboration, Constraints on Higgs boson production with large transverse momentum using  $H \rightarrow b\bar{b}$  decays in the ATLAS detector, *Phys. Rev. D* **105**, 092003 (2022).
- [42] S. Frixione, E. Laenen, P. Motylinski, C. White, and B. R. Webber, Single-top hadroproduction in association with a  $W$  boson, *J. High Energy Phys.* **07** (2008) 029.
- [43] D. J. Lange, The EvtGen particle decay simulation package, *Nucl. Instrum. Methods Phys. Res., Sect. A* **462**, 152 (2001).
- [44] ATLAS Collaboration, Vertex reconstruction performance of the ATLAS detector at  $\sqrt{s} = 13$  TeV, Report No. ATL-PHYS-PUB-2015-026, 2015, <https://cds.cern.ch/record/2037717>.
- [45] ATLAS Collaboration, Selection of jets produced in 13 TeV proton–proton collisions with the ATLAS detector, Report No. ATLAS-CONF-2015-029, 2015, <https://cds.cern.ch/record/2037702>.
- [46] M. Cacciari, G. P. Salam, and G. Soyez, The anti- $k_r$  jet clustering algorithm, *J. High Energy Phys.* **04** (2008) 063.
- [47] M. Cacciari, G. P. Salam, and G. Soyez, FastJet user manual, *Eur. Phys. J. C* **72**, 1896 (2012).
- [48] ATLAS Collaboration, Topological cell clustering in the ATLAS calorimeters and its performance in LHC Run 1, *Eur. Phys. J. C* **77**, 490 (2017).
- [49] D. Krohn, J. Thaler, and L.-T. Wang, Jet trimming, *J. High Energy Phys.* **02** (2010) 084.
- [50] ATLAS Collaboration, In situ calibration of large-radius jet energy and mass in 13 TeV proton–proton collisions with the ATLAS detector, *Eur. Phys. J. C* **79**, 135 (2019).
- [51] ATLAS Collaboration, Variable radius, exclusive- $k_T$ , and center-of-mass subjet reconstruction for Higgs( $\rightarrow b\bar{b}$ ) tagging in ATLAS, Report No. ATL-PHYS-PUB-2017-010, 2017, <https://cds.cern.ch/record/2268678>.
- [52] M. Cacciari, G. P. Salam, and G. Soyez, The catchment area of jets, *J. High Energy Phys.* **04** (2008) 005.
- [53] ATLAS Collaboration, Electron and photon performance measurements with the ATLAS detector using the 2015–2017 LHC proton–proton collision data, *J. Instrum.* **14**, P12006 (2019).
- [54] ATLAS Collaboration, Muon reconstruction and identification efficiency in ATLAS using the full Run 2  $pp$  collision data set at  $\sqrt{s} = 13$  TeV, *Eur. Phys. J. C* **81**, 578 (2021).
- [55] A. J. Larkoski, I. Moulton, and D. Neill, Power counting to better jet observables, *J. High Energy Phys.* **12** (2014) 009.
- [56] A. J. Larkoski, I. Moulton, and D. Neill, Analytic boosted boson discrimination, *J. High Energy Phys.* **05** (2016) 117.
- [57] ATLAS Collaboration, Boosted hadronic vector boson and top quark tagging with ATLAS using Run 2 data, Report No. ATL-PHYS-PUB-2020-017, 2020, <https://cds.cern.ch/record/2724149>.
- [58] ATLAS Collaboration, Identification of boosted Higgs bosons decaying into  $b\bar{b}$  with neural networks and variable radius subjects in ATLAS, ATL-PHYS-PUB-2020-019, 2020, <https://cds.cern.ch/record/2724739>.
- [59] ATLAS Collaboration, Identification of boosted Higgs bosons decaying into  $b$ -quark pairs with the ATLAS detector at 13 TeV, *Eur. Phys. J. C* **79**, 836 (2019).
- [60] ATLAS Collaboration, Search for resonances decaying into a weak vector boson and a Higgs boson in the fully hadronic final state produced in proton–proton collisions at  $\sqrt{s} = 13$  TeV with the ATLAS detector, *Phys. Rev. D* **102**, 112008 (2020).
- [61] ATLAS Collaboration, Measurements of  $t\bar{t}$  differential cross-sections of highly boosted top quarks decaying to



all-hadronic final states in  $pp$  collisions at  $\sqrt{s} = 13$  TeV using the ATLAS detector, *Phys. Rev. D* **98**, 012003 (2018).

[62] ATLAS Collaboration, Performance of top-quark and  $W$ -boson tagging with ATLAS in Run 2 of the LHC, *Eur. Phys. J. C* **79**, 375 (2019).

[63] ATLAS Collaboration, Efficiency corrections for a tagger for boosted  $H \rightarrow b\bar{b}$  decays in  $pp$  collisions at  $\sqrt{s} = 13$  TeV with the ATLAS detector, Report No. ATL-PHYS-PUB-2021-035, 2021, <https://cds.cern.ch/record/2777811>.

[64] ATLAS Collaboration, Luminosity determination in  $pp$  collisions at  $\sqrt{s} = 13$  TeV using the ATLAS detector at the LHC, *Eur. Phys. J. C* **83**, 982 (2023).

[65] M. Kendall and A. Stuart, *The Advanced Theory of Statistics, Volume 2: Inference and Relationship* (Charles Griffin, London, 1961).

[66] G. Cowan, K. Cranmer, E. Gross, and O. Vitells, Asymptotic formulae for likelihood-based tests of new physics, *Eur. Phys. J. C* **71**, 1554 (2011); *Eur. Phys. J. C* **73**, 2501 (2013).

[67] M. Cepeda *et al.*, Higgs Physics at the HL-LHC and HE-LHC, CERN Yellow Rep. Monogr. **7**, 221 (2019), 10.23731/CYRM-2019-007.221.

[68] ATLAS Collaboration, ATLAS computing acknowledgements, Report No. ATL-SOFT-PUB-2023-001, 2023, <https://cds.cern.ch/record/2869272>.

G. Aad<sup>102</sup>, B. Abbott<sup>120</sup>, K. Abeling<sup>55</sup>, N. J. Abicht<sup>49</sup>, S. H. Abidi<sup>29</sup>, A. Aboulhorma<sup>35e</sup>, H. Abramowicz<sup>151</sup>, H. Abreu<sup>150</sup>, Y. Abulaiti<sup>117</sup>, B. S. Acharya<sup>69a,69b,b</sup>, C. Adam Bourdarios<sup>4</sup>, L. Adamczyk<sup>86a</sup>, S. V. Addepalli<sup>26</sup>, M. J. Addison<sup>101</sup>, J. Adelman<sup>115</sup>, A. Adiguzel<sup>21c</sup>, T. Adye<sup>134</sup>, A. A. Affolder<sup>136</sup>, Y. Afik<sup>39</sup>, M. N. Agaras<sup>13</sup>, J. Agarwala<sup>73a,73b</sup>, A. Aggarwal<sup>100</sup>, C. Agheorghiesei<sup>27c</sup>, A. Ahmad<sup>36</sup>, F. Ahmadov<sup>38,c</sup>, W. S. Ahmed<sup>104</sup>, S. Ahuja<sup>95</sup>, X. Ai<sup>62e</sup>, G. Aielli<sup>76a,76b</sup>, A. Aikot<sup>163</sup>, M. Ait Tamlihat<sup>35e</sup>, B. Aitbenkikh<sup>35a</sup>, I. Aizenberg<sup>169</sup>, M. Akbiyik<sup>100</sup>, T. P. A. Åkesson<sup>98</sup>, A. V. Akimov<sup>37</sup>, D. Akiyama<sup>168</sup>, N. N. Akolkar<sup>24</sup>, S. Aktas<sup>21a</sup>, K. Al Khoury<sup>41</sup>, G. L. Alberghi<sup>23b</sup>, J. Albert<sup>165</sup>, P. Albicocco<sup>53</sup>, G. L. Albouy<sup>60</sup>, S. Alderweireldt<sup>52</sup>, Z. L. Alegria<sup>121</sup>, M. Aleksa<sup>36</sup>, I. N. Aleksandrov<sup>38</sup>, C. Alexa<sup>27b</sup>, T. Alexopoulos<sup>10</sup>, F. Alfonsi<sup>23b</sup>, M. Algren<sup>56</sup>, M. Alhroob<sup>120</sup>, B. Ali<sup>132</sup>, H. M. J. Ali<sup>91</sup>, S. Ali<sup>148</sup>, S. W. Alibocus<sup>92</sup>, M. Aliev<sup>145</sup>, G. Alimonti<sup>71a</sup>, W. Alkahi<sup>55</sup>, C. Allaire<sup>66</sup>, B. M. M. Allbrooke<sup>146</sup>, J. F. Allen<sup>52</sup>, C. A. Allendes Flores<sup>137f</sup>, P. P. Allport<sup>20</sup>, A. Aloisio<sup>72a,72b</sup>, F. Alonso<sup>90</sup>, C. Alpigiani<sup>138</sup>, M. Alvarez Estevez<sup>99</sup>, A. Alvarez Fernandez<sup>100</sup>, M. Alves Cardoso<sup>56</sup>, M. G. Alviggi<sup>72a,72b</sup>, M. Aly<sup>101</sup>, Y. Amaral Coutinho<sup>83b</sup>, A. Ambler<sup>104</sup>, C. Amelung<sup>36</sup>, M. Amerl<sup>101</sup>, C. G. Ames<sup>109</sup>, D. Amidei<sup>106</sup>, S. P. Amor Dos Santos<sup>130a</sup>, K. R. Amos<sup>163</sup>, V. Ananiev<sup>125</sup>, C. Anastopoulos<sup>139</sup>, T. Andeen<sup>11</sup>, J. K. Anders<sup>36</sup>, S. Y. Andreato<sup>47a,47b</sup>, A. Andreatza<sup>71a,71b</sup>, S. Angelidakis<sup>9</sup>, A. Angerami<sup>41,d</sup>, A. V. Anisenkov<sup>37</sup>, A. Annovi<sup>74a</sup>, C. Antel<sup>56</sup>, M. T. Anthony<sup>139</sup>, E. Antipov<sup>145</sup>, M. Antonelli<sup>53</sup>, F. Anulli<sup>75a</sup>, M. Aoki<sup>84</sup>, T. Aoki<sup>153</sup>, J. A. Aparisi Pozo<sup>163</sup>, M. A. Aparo<sup>146</sup>, L. Aperio Bella<sup>48</sup>, C. Appelt<sup>18</sup>, A. Apyan<sup>26</sup>, N. Aranzabal<sup>36</sup>, S. J. Arbiol Val<sup>87</sup>, C. Arcangeletti<sup>53</sup>, A. T. H. Arce<sup>51</sup>, E. Arena<sup>92</sup>, J-F. Arguin<sup>108</sup>, S. Argyropoulos<sup>54</sup>, J.-H. Arling<sup>48</sup>, O. Arnaez<sup>4</sup>, H. Arnold<sup>114</sup>, G. Artoni<sup>75a,75b</sup>, H. Asada<sup>111</sup>, K. Asai<sup>118</sup>, S. Asai<sup>153</sup>, N. A. Asbah<sup>61</sup>, K. Assamagan<sup>29</sup>, R. Astalos<sup>28a</sup>, S. Atashi<sup>159</sup>, R. J. Atkin<sup>33a</sup>, M. Atkinson<sup>162</sup>, H. Atmani<sup>35f</sup>, P. A. Atmasiddha<sup>128</sup>, K. Augsten<sup>132</sup>, S. Auricchio<sup>72a,72b</sup>, A. D. Auriol<sup>20</sup>, V. A. Austrup<sup>101</sup>, G. Avolio<sup>36</sup>, K. Axiotis<sup>56</sup>, G. Azuelos<sup>108,e</sup>, D. Babal<sup>28b</sup>, H. Bachacou<sup>135</sup>, K. Bachas<sup>152,f</sup>, A. Bachiu<sup>34</sup>, F. Backman<sup>47a,47b</sup>, A. Badea<sup>61</sup>, T. M. Baer<sup>106</sup>, P. Bagnaia<sup>75a,75b</sup>, M. Bahmani<sup>18</sup>, D. Bahner<sup>54</sup>, A. J. Bailey<sup>163</sup>, V. R. Bailey<sup>162</sup>, J. T. Baines<sup>134</sup>, L. Baines<sup>94</sup>, O. K. Baker<sup>172</sup>, E. Bakos<sup>15</sup>, D. Bakshi Gupta<sup>8</sup>, V. Balakrishnan<sup>120</sup>, R. Balasubramanian<sup>114</sup>, E. M. Baldin<sup>37</sup>, P. Balek<sup>86a</sup>, E. Ballabene<sup>23b,23a</sup>, F. Balli<sup>135</sup>, L. M. Baltes<sup>63a</sup>, W. K. Balunas<sup>32</sup>, J. Balz<sup>100</sup>, E. Banas<sup>87</sup>, M. Bandieramonte<sup>129</sup>, A. Bandyopadhyay<sup>24</sup>, S. Bansal<sup>24</sup>, L. Barak<sup>151</sup>, M. Barakat<sup>48</sup>, E. L. Barberio<sup>105</sup>, D. Barberis<sup>57b,57a</sup>, M. Barbero<sup>102</sup>, M. Z. Barel<sup>114</sup>, K. N. Barends<sup>33a</sup>, T. Barillari<sup>110</sup>, M.-S. Barisits<sup>36</sup>, T. Barklow<sup>143</sup>, P. Baron<sup>122</sup>, D. A. Baron Moreno<sup>101</sup>, A. Baroncelli<sup>62a</sup>, G. Barone<sup>29</sup>, A. J. Barr<sup>126</sup>, J. D. Barr<sup>96</sup>, L. Barranco Navarro<sup>47a,47b</sup>, F. Barreiro<sup>99</sup>, J. Barreiro Guimarães da Costa<sup>14a</sup>, U. Barron<sup>151</sup>, M. G. Barros Teixeira<sup>130a</sup>, S. Barsov<sup>37</sup>, F. Bartels<sup>63a</sup>, R. Bartoldus<sup>143</sup>, A. E. Barton<sup>91</sup>, P. Bartos<sup>28a</sup>, A. Basan<sup>100</sup>, M. Baselga<sup>49</sup>, A. Bassalat<sup>66,g</sup>, M. J. Basso<sup>156a</sup>, C. R. Basson<sup>101</sup>, R. L. Bates<sup>59</sup>, S. Batlamous<sup>35e</sup>, J. R. Batley<sup>32</sup>, B. Batool<sup>141</sup>, M. Battaglia<sup>136</sup>, D. Battulga<sup>18</sup>, M. Bauce<sup>75a,75b</sup>, M. Bauer<sup>36</sup>, P. Bauer<sup>24</sup>, L. T. Bazzano Hurrell<sup>30</sup>, J. B. Beacham<sup>51</sup>, T. Beau<sup>127</sup>, J. Y. Beauchamp<sup>90</sup>, P. H. Beauchemin<sup>158</sup>, P. Bechtel<sup>24</sup>, H. P. Beck<sup>19,h</sup>, K. Becker<sup>167</sup>, A. J. Beddall<sup>82</sup>, V. A. Bednyakov<sup>38</sup>, C. P. Bee<sup>145</sup>, L. J. Beemster<sup>15</sup>, T. A. Beermann<sup>36</sup>, M. Begalli<sup>83d</sup>, M. Begel<sup>29</sup>, A. Behera<sup>145</sup>, J. K. Behr<sup>48</sup>, J. F. Beirer<sup>36</sup>, F. Beisiegel<sup>24</sup>, M. Belfkir<sup>116b</sup>, G. Bella<sup>151</sup>, L. Bellagamba<sup>23b</sup>, A. Bellerive<sup>34</sup>



















M. Wobisch<sup>97</sup>, Z. Wolffs<sup>114</sup>, J. Wollrath<sup>159</sup>, M. W. Wolter<sup>87</sup>, H. Wolters<sup>130a,130c</sup>, A. F. Wongel<sup>48</sup>,  
 E. L. Woodward<sup>41</sup>, S. D. Worm<sup>48</sup>, B. K. Wosiek<sup>87</sup>, K. W. Woźniak<sup>87</sup>, S. Wozniowski<sup>55</sup>, K. Wraight<sup>59</sup>, C. Wu<sup>20</sup>,  
 J. Wu<sup>14a,14e</sup>, M. Wu<sup>64a</sup>, M. Wu<sup>113</sup>, S. L. Wu<sup>170</sup>, X. Wu<sup>56</sup>, Y. Wu<sup>62a</sup>, Z. Wu<sup>135</sup>, J. Wuerzinger<sup>110,w</sup>,  
 T. R. Wyatt<sup>101</sup>, B. M. Wynne<sup>52</sup>, S. Xella<sup>42</sup>, L. Xia<sup>14c</sup>, M. Xia<sup>14b</sup>, J. Xiang<sup>64c</sup>, M. Xie<sup>62a</sup>, X. Xie<sup>62a</sup>,  
 S. Xin<sup>14a,14e</sup>, A. Xiong<sup>123</sup>, J. Xiong<sup>17a</sup>, D. Xu<sup>14a</sup>, H. Xu<sup>62a</sup>, L. Xu<sup>62a</sup>, R. Xu<sup>128</sup>, T. Xu<sup>106</sup>, Y. Xu<sup>14b</sup>, Z. Xu<sup>52</sup>,  
 Z. Xu<sup>14c</sup>, B. Yabsley<sup>147</sup>, S. Yacoob<sup>33a</sup>, Y. Yamaguchi<sup>154</sup>, E. Yamashita<sup>153</sup>, H. Yamauchi<sup>157</sup>, T. Yamazaki<sup>17a</sup>,  
 Y. Yamazaki<sup>85</sup>, J. Yan<sup>62c</sup>, S. Yan<sup>126</sup>, Z. Yan<sup>25</sup>, H. J. Yang<sup>62c,62d</sup>, H. T. Yang<sup>62a</sup>, S. Yang<sup>62a</sup>, T. Yang<sup>64c</sup>,  
 X. Yang<sup>36</sup>, X. Yang<sup>14a</sup>, Y. Yang<sup>44</sup>, Y. Yang<sup>62a</sup>, Z. Yang<sup>62a</sup>, W-M. Yao<sup>17a</sup>, Y. C. Yap<sup>48</sup>, H. Ye<sup>14c</sup>, H. Ye<sup>55</sup>,  
 J. Ye<sup>14a</sup>, S. Ye<sup>29</sup>, X. Ye<sup>62a</sup>, Y. Yeh<sup>96</sup>, I. Yeletsikh<sup>38</sup>, B. K. Yeo<sup>17b</sup>, M. R. Yexley<sup>96</sup>, P. Yin<sup>41</sup>, K. Yorita<sup>168</sup>,  
 S. Younas<sup>27b</sup>, C. J. S. Young<sup>36</sup>, C. Young<sup>143</sup>, C. Yu<sup>14a,14e,mm</sup>, Y. Yu<sup>62a</sup>, M. Yuan<sup>106</sup>, R. Yuan<sup>62b</sup>, L. Yue<sup>96</sup>,  
 M. Zaazoua<sup>62a</sup>, B. Zabinski<sup>87</sup>, E. Zaid<sup>52</sup>, Z. K. Zak<sup>87</sup>, T. Zakareishvili<sup>149b</sup>, N. Zakharchuk<sup>34</sup>, S. Zambito<sup>56</sup>,  
 J. A. Zamora Saa<sup>137d,137b</sup>, J. Zang<sup>153</sup>, D. Zanzi<sup>54</sup>, O. Zaplatilek<sup>132</sup>, C. Zeitnitz<sup>171</sup>, H. Zeng<sup>14a</sup>, J. C. Zeng<sup>162</sup>,  
 D. T. Zenger Jr.<sup>26</sup>, O. Zenin<sup>37</sup>, T. Ženiš<sup>28a</sup>, S. Zenz<sup>94</sup>, S. Zerradi<sup>35a</sup>, D. Zerwas<sup>66</sup>, M. Zhai<sup>14a,14e</sup>, B. Zhang<sup>14c</sup>,  
 D. F. Zhang<sup>139</sup>, J. Zhang<sup>62b</sup>, J. Zhang<sup>6</sup>, K. Zhang<sup>14a,14e</sup>, L. Zhang<sup>14c</sup>, P. Zhang<sup>14a,14e</sup>, R. Zhang<sup>170</sup>, S. Zhang<sup>106</sup>,  
 S. Zhang<sup>44</sup>, T. Zhang<sup>153</sup>, X. Zhang<sup>62c</sup>, X. Zhang<sup>62b</sup>, Y. Zhang<sup>62c,5</sup>, Y. Zhang<sup>96</sup>, Y. Zhang<sup>14c</sup>, Z. Zhang<sup>17a</sup>,  
 Z. Zhang<sup>66</sup>, H. Zhao<sup>138</sup>, T. Zhao<sup>62b</sup>, Y. Zhao<sup>136</sup>, Z. Zhao<sup>62a</sup>, A. Zhemchugov<sup>38</sup>, J. Zheng<sup>14c</sup>, K. Zheng<sup>162</sup>,  
 X. Zheng<sup>62a</sup>, Z. Zheng<sup>143</sup>, D. Zhong<sup>162</sup>, B. Zhou<sup>106</sup>, H. Zhou<sup>7</sup>, N. Zhou<sup>62c</sup>, Y. Zhou<sup>14c</sup>, Y. Zhou<sup>7</sup>, C. G. Zhu<sup>62b</sup>,  
 J. Zhu<sup>106</sup>, Y. Zhu<sup>62c</sup>, Y. Zhu<sup>62a</sup>, X. Zhuang<sup>14a</sup>, K. Zhukov<sup>37</sup>, V. Zhulanov<sup>37</sup>, N. I. Zimine<sup>38</sup>, J. Zinsser<sup>63b</sup>,  
 M. Ziolkowski<sup>141</sup>, L. Živković<sup>15</sup>, A. Zoccoli<sup>23b,23a</sup>, K. Zoch<sup>61</sup>, T. G. Zorbas<sup>139</sup>, O. Zormpa<sup>46</sup>, W. Zou<sup>41</sup>, and  
 L. Zwalinski<sup>36</sup>

(ATLAS Collaboration)

- <sup>1</sup>Department of Physics, University of Adelaide, Adelaide, Australia  
<sup>2</sup>Department of Physics, University of Alberta, Edmonton, Alberta, Canada  
<sup>3a</sup>Department of Physics, Ankara University, Ankara, Türkiye  
<sup>3b</sup>Division of Physics, TOBB University of Economics and Technology, Ankara, Türkiye  
<sup>4</sup>LAPP, Université Savoie Mont Blanc, CNRS/IN2P3, Annecy, France  
<sup>5</sup>APC, Université Paris Cité, CNRS/IN2P3, Paris, France  
<sup>6</sup>High Energy Physics Division, Argonne National Laboratory, Argonne, Illinois, USA  
<sup>7</sup>Department of Physics, University of Arizona, Tucson, Arizona, USA  
<sup>8</sup>Department of Physics, University of Texas at Arlington, Arlington, Texas, USA  
<sup>9</sup>Physics Department, National and Kapodistrian University of Athens, Athens, Greece  
<sup>10</sup>Physics Department, National Technical University of Athens, Zografou, Greece  
<sup>11</sup>Department of Physics, University of Texas at Austin, Austin, Texas, USA  
<sup>12</sup>Institute of Physics, Azerbaijan Academy of Sciences, Baku, Azerbaijan  
<sup>13</sup>Institut de Física d'Altes Energies (IFAE), Barcelona Institute of Science and Technology, Barcelona, Spain  
<sup>14a</sup>Institute of High Energy Physics, Chinese Academy of Sciences, Beijing, China  
<sup>14b</sup>Physics Department, Tsinghua University, Beijing, China  
<sup>14c</sup>Department of Physics, Nanjing University, Nanjing, China  
<sup>14d</sup>School of Science, Shenzhen Campus of Sun Yat-sen University, China  
<sup>14e</sup>University of Chinese Academy of Science (UCAS), Beijing, China  
<sup>15</sup>Institute of Physics, University of Belgrade, Belgrade, Serbia  
<sup>16</sup>Department for Physics and Technology, University of Bergen, Bergen, Norway  
<sup>17a</sup>Physics Division, Lawrence Berkeley National Laboratory, Berkeley, California, USA  
<sup>17b</sup>University of California, Berkeley, California, USA  
<sup>18</sup>Institut für Physik, Humboldt Universität zu Berlin, Berlin, Germany  
<sup>19</sup>Albert Einstein Center for Fundamental Physics and Laboratory for High Energy Physics, University of Bern, Bern, Switzerland  
<sup>20</sup>School of Physics and Astronomy, University of Birmingham, Birmingham, United Kingdom  
<sup>21a</sup>Department of Physics, Bogazici University, Istanbul, Türkiye  
<sup>21b</sup>Department of Physics Engineering, Gaziantep University, Gaziantep, Türkiye  
<sup>21c</sup>Department of Physics, Istanbul University, Istanbul, Türkiye  
<sup>22a</sup>Facultad de Ciencias y Centro de Investigaciones, Universidad Antonio Nariño, Bogotá, Colombia

- <sup>22b</sup>*Departamento de Física, Universidad Nacional de Colombia, Bogotá, Colombia*
- <sup>23a</sup>*Dipartimento di Fisica e Astronomia A. Righi, Università di Bologna, Bologna, Italy*  
<sup>23b</sup>*INFN Sezione di Bologna, Italy*
- <sup>24</sup>*Physikalisches Institut, Universität Bonn, Bonn, Germany*
- <sup>25</sup>*Department of Physics, Boston University, Boston, Massachusetts, USA*
- <sup>26</sup>*Department of Physics, Brandeis University, Waltham, Massachusetts, USA*
- <sup>27a</sup>*Transilvania University of Brasov, Brasov, Romania*
- <sup>27b</sup>*Horia Hulubei National Institute of Physics and Nuclear Engineering, Bucharest, Romania*
- <sup>27c</sup>*Department of Physics, Alexandru Ioan Cuza University of Iasi, Iasi, Romania*
- <sup>27d</sup>*National Institute for Research and Development of Isotopic and Molecular Technologies, Physics Department, Cluj-Napoca, Romania*
- <sup>27e</sup>*National University of Science and Technology Politehnica, Bucharest, Romania*
- <sup>27f</sup>*West University in Timisoara, Timisoara, Romania*
- <sup>27g</sup>*Faculty of Physics, University of Bucharest, Bucharest, Romania*
- <sup>28a</sup>*Faculty of Mathematics, Physics and Informatics, Comenius University, Bratislava, Slovak Republic*
- <sup>28b</sup>*Department of Subnuclear Physics, Institute of Experimental Physics of the Slovak Academy of Sciences, Kosice, Slovak Republic*
- <sup>29</sup>*Physics Department, Brookhaven National Laboratory, Upton, New York, USA*
- <sup>30</sup>*Universidad de Buenos Aires, Facultad de Ciencias Exactas y Naturales, Departamento de Física, y CONICET, Instituto de Física de Buenos Aires (IFIBA), Buenos Aires, Argentina*
- <sup>31</sup>*California State University, California, USA*
- <sup>32</sup>*Cavendish Laboratory, University of Cambridge, Cambridge, United Kingdom*
- <sup>33a</sup>*Department of Physics, University of Cape Town, Cape Town, South Africa*
- <sup>33b</sup>*iThemba Labs, Western Cape, South Africa*
- <sup>33c</sup>*Department of Mechanical Engineering Science, University of Johannesburg, Johannesburg, South Africa*
- <sup>33d</sup>*National Institute of Physics, University of the Philippines Diliman (Philippines), Philippines*
- <sup>33e</sup>*University of South Africa, Department of Physics, Pretoria, South Africa*
- <sup>33f</sup>*University of Zululand, KwaDlangezwa, South Africa*
- <sup>33g</sup>*School of Physics, University of the Witwatersrand, Johannesburg, South Africa*
- <sup>34</sup>*Department of Physics, Carleton University, Ottawa, Ontario, Canada*
- <sup>35a</sup>*Faculté des Sciences Ain Chock, Réseau Universitaire de Physique des Hautes Energies - Université Hassan II, Casablanca, Morocco*
- <sup>35b</sup>*Faculté des Sciences, Université Ibn-Tofail, Kénitra, Morocco*
- <sup>35c</sup>*Faculté des Sciences Semlalia, Université Cadi Ayyad, LPHEA-Marrakech, Morocco*
- <sup>35d</sup>*LPMR, Faculté des Sciences, Université Mohammed Premier, Oujda, Morocco*
- <sup>35e</sup>*Faculté des sciences, Université Mohammed V, Rabat, Morocco*
- <sup>35f</sup>*Institute of Applied Physics, Mohammed VI Polytechnic University, Ben Guerir, Morocco*
- <sup>36</sup>*CERN, Geneva, Switzerland*
- <sup>37</sup>*Affiliated with an institute covered by a cooperation agreement with CERN*
- <sup>38</sup>*Affiliated with an international laboratory covered by a cooperation agreement with CERN*
- <sup>39</sup>*Enrico Fermi Institute, University of Chicago, Chicago, Illinois, USA*
- <sup>40</sup>*LPC, Université Clermont Auvergne, CNRS/IN2P3, Clermont-Ferrand, France*
- <sup>41</sup>*Nevis Laboratory, Columbia University, Irvington, New York, USA*
- <sup>42</sup>*Niels Bohr Institute, University of Copenhagen, Copenhagen, Denmark*
- <sup>43a</sup>*Dipartimento di Fisica, Università della Calabria, Rende, Italy*
- <sup>43b</sup>*INFN Gruppo Collegato di Cosenza, Laboratori Nazionali di Frascati, Italy*
- <sup>44</sup>*Physics Department, Southern Methodist University, Dallas, Texas, USA*
- <sup>45</sup>*Physics Department, University of Texas at Dallas, Richardson, Texas, USA*
- <sup>46</sup>*National Centre for Scientific Research “Demokritos”, Agia Paraskevi, Greece*
- <sup>47a</sup>*Department of Physics, Stockholm University, Sweden*
- <sup>47b</sup>*Oskar Klein Centre, Stockholm, Sweden*
- <sup>48</sup>*Deutsches Elektronen-Synchrotron DESY, Hamburg and Zeuthen, Germany*
- <sup>49</sup>*Fakultät Physik, Technische Universität Dortmund, Dortmund, Germany*
- <sup>50</sup>*Institut für Kern- und Teilchenphysik, Technische Universität Dresden, Dresden, Germany*
- <sup>51</sup>*Department of Physics, Duke University, Durham, North Carolina, USA*
- <sup>52</sup>*SUPA - School of Physics and Astronomy, University of Edinburgh, Edinburgh, United Kingdom*
- <sup>53</sup>*INFN e Laboratori Nazionali di Frascati, Frascati, Italy*
- <sup>54</sup>*Physikalisches Institut, Albert-Ludwigs-Universität Freiburg, Freiburg, Germany*
- <sup>55</sup>*II. Physikalisches Institut, Georg-August-Universität Göttingen, Göttingen, Germany*
- <sup>56</sup>*Département de Physique Nucléaire et Corpusculaire, Université de Genève, Genève, Switzerland*

- <sup>57a</sup>*Dipartimento di Fisica, Università di Genova, Genova, Italy*  
<sup>57b</sup>*INFN Sezione di Genova, Italy*
- <sup>58</sup>*II. Physikalisches Institut, Justus-Liebig-Universität Giessen, Giessen, Germany*
- <sup>59</sup>*SUPA - School of Physics and Astronomy, University of Glasgow, Glasgow, United Kingdom*
- <sup>60</sup>*LPSC, Université Grenoble Alpes, CNRS/IN2P3, Grenoble INP, Grenoble, France*
- <sup>61</sup>*Laboratory for Particle Physics and Cosmology, Harvard University, Cambridge, Massachusetts, USA*
- <sup>62a</sup>*Department of Modern Physics and State Key Laboratory of Particle Detection and Electronics, University of Science and Technology of China, Hefei, China*
- <sup>62b</sup>*Institute of Frontier and Interdisciplinary Science and Key Laboratory of Particle Physics and Particle Irradiation (MOE), Shandong University, Qingdao, China*
- <sup>62c</sup>*School of Physics and Astronomy, Shanghai Jiao Tong University, Key Laboratory for Particle Astrophysics and Cosmology (MOE), SKLPPC, Shanghai, China*  
<sup>62d</sup>*Tsung-Dao Lee Institute, Shanghai, China*
- <sup>62e</sup>*School of Physics and Microelectronics, Zhengzhou University, China*
- <sup>63a</sup>*Kirchhoff-Institut für Physik, Ruprecht-Karls-Universität Heidelberg, Heidelberg, Germany*
- <sup>63b</sup>*Physikalisches Institut, Ruprecht-Karls-Universität Heidelberg, Heidelberg, Germany*
- <sup>64a</sup>*Department of Physics, Chinese University of Hong Kong, Shatin, N.T., Hong Kong, China*
- <sup>64b</sup>*Department of Physics, University of Hong Kong, Hong Kong, China*
- <sup>64c</sup>*Department of Physics and Institute for Advanced Study, Hong Kong University of Science and Technology, Clear Water Bay, Kowloon, Hong Kong, China*
- <sup>65</sup>*Department of Physics, National Tsing Hua University, Hsinchu, Taiwan*
- <sup>66</sup>*IJCLab, Université Paris-Saclay, CNRS/IN2P3, 91405, Orsay, France*
- <sup>67</sup>*Centro Nacional de Microelectrónica (IMB-CNM-CSIC), Barcelona, Spain*
- <sup>68</sup>*Department of Physics, Indiana University, Bloomington, Indiana, USA*
- <sup>69a</sup>*INFN Gruppo Collegato di Udine, Sezione di Trieste, Udine, Italy*  
<sup>69b</sup>*ICTP, Trieste, Italy*
- <sup>69c</sup>*Dipartimento Politecnico di Ingegneria e Architettura, Università di Udine, Udine, Italy*  
<sup>70a</sup>*INFN Sezione di Lecce, Italy*
- <sup>70b</sup>*Dipartimento di Matematica e Fisica, Università del Salento, Lecce, Italy*  
<sup>71a</sup>*INFN Sezione di Milano, Italy*
- <sup>71b</sup>*Dipartimento di Fisica, Università di Milano, Milano, Italy*  
<sup>72a</sup>*INFN Sezione di Napoli, Italy*
- <sup>72b</sup>*Dipartimento di Fisica, Università di Napoli, Napoli, Italy*  
<sup>73a</sup>*INFN Sezione di Pavia, Italy*
- <sup>73b</sup>*Dipartimento di Fisica, Università di Pavia, Pavia, Italy*  
<sup>74a</sup>*INFN Sezione di Pisa, Italy*
- <sup>74b</sup>*Dipartimento di Fisica E. Fermi, Università di Pisa, Pisa, Italy*  
<sup>75a</sup>*INFN Sezione di Roma, Italy*
- <sup>75b</sup>*Dipartimento di Fisica, Sapienza Università di Roma, Roma, Italy*  
<sup>76a</sup>*INFN Sezione di Roma Tor Vergata, Italy*
- <sup>76b</sup>*Dipartimento di Fisica, Università di Roma Tor Vergata, Roma, Italy*  
<sup>77a</sup>*INFN Sezione di Roma Tre, Italy*
- <sup>77b</sup>*Dipartimento di Matematica e Fisica, Università Roma Tre, Roma, Italy*  
<sup>78a</sup>*INFN-TIFPA, Italy*
- <sup>78b</sup>*Università degli Studi di Trento, Trento, Italy*
- <sup>79</sup>*Universität Innsbruck, Department of Astro and Particle Physics, Innsbruck, Austria*
- <sup>80</sup>*University of Iowa, Iowa City, Iowa, USA*
- <sup>81</sup>*Department of Physics and Astronomy, Iowa State University, Ames, Iowa, USA*
- <sup>82</sup>*Istinye University, Sariyer, Istanbul, Türkiye*
- <sup>83a</sup>*Departamento de Engenharia Elétrica, Universidade Federal de Juiz de Fora (UFJF), Juiz de Fora, Brazil*
- <sup>83b</sup>*Universidade Federal do Rio De Janeiro COPPE/EE/IF, Rio de Janeiro, Brazil*
- <sup>83c</sup>*Instituto de Física, Universidade de São Paulo, São Paulo, Brazil*  
<sup>83d</sup>*Rio de Janeiro State University, Rio de Janeiro, Brazil*
- <sup>84</sup>*KEK, High Energy Accelerator Research Organization, Tsukuba, Japan*  
<sup>85</sup>*Graduate School of Science, Kobe University, Kobe, Japan*
- <sup>86a</sup>*AGH University of Krakow, Faculty of Physics and Applied Computer Science, Krakow, Poland*  
<sup>86b</sup>*Marian Smoluchowski Institute of Physics, Jagiellonian University, Krakow, Poland*
- <sup>87</sup>*Institute of Nuclear Physics Polish Academy of Sciences, Krakow, Poland*  
<sup>88</sup>*Faculty of Science, Kyoto University, Kyoto, Japan*
- <sup>89</sup>*Research Center for Advanced Particle Physics and Department of Physics, Kyushu University, Fukuoka, Japan*

- <sup>90</sup>*Instituto de Física La Plata, Universidad Nacional de La Plata and CONICET, La Plata, Argentina*
- <sup>91</sup>*Physics Department, Lancaster University, Lancaster, United Kingdom*
- <sup>92</sup>*Oliver Lodge Laboratory, University of Liverpool, Liverpool, United Kingdom*
- <sup>93</sup>*Department of Experimental Particle Physics, Jožef Stefan Institute and Department of Physics, University of Ljubljana, Ljubljana, Slovenia*
- <sup>94</sup>*School of Physics and Astronomy, Queen Mary University of London, London, United Kingdom*
- <sup>95</sup>*Department of Physics, Royal Holloway University of London, Egham, United Kingdom*
- <sup>96</sup>*Department of Physics and Astronomy, University College London, London, United Kingdom*
- <sup>97</sup>*Louisiana Tech University, Ruston, Louisiana, USA*
- <sup>98</sup>*Fysiska institutionen, Lunds universitet, Lund, Sweden*
- <sup>99</sup>*Departamento de Física Teórica C-15 and CIAFF, Universidad Autónoma de Madrid, Madrid, Spain*
- <sup>100</sup>*Institut für Physik, Universität Mainz, Mainz, Germany*
- <sup>101</sup>*School of Physics and Astronomy, University of Manchester, Manchester, United Kingdom*
- <sup>102</sup>*CPPM, Aix-Marseille Université, CNRS/IN2P3, Marseille, France*
- <sup>103</sup>*Department of Physics, University of Massachusetts, Amherst, Massachusetts, USA*
- <sup>104</sup>*Department of Physics, McGill University, Montreal, Quebec, Canada*
- <sup>105</sup>*School of Physics, University of Melbourne, Victoria, Australia*
- <sup>106</sup>*Department of Physics, University of Michigan, Ann Arbor, Michigan, USA*
- <sup>107</sup>*Department of Physics and Astronomy, Michigan State University, East Lansing, Michigan, USA*
- <sup>108</sup>*Group of Particle Physics, University of Montreal, Montreal, Quebec, Canada*
- <sup>109</sup>*Fakultät für Physik, Ludwig-Maximilians-Universität München, München, Germany*
- <sup>110</sup>*Max-Planck-Institut für Physik (Werner-Heisenberg-Institut), München, Germany*
- <sup>111</sup>*Graduate School of Science and Kobayashi-Maskawa Institute, Nagoya University, Nagoya, Japan*
- <sup>112</sup>*Department of Physics and Astronomy, University of New Mexico, Albuquerque, New Mexico, USA*
- <sup>113</sup>*Institute for Mathematics, Astrophysics and Particle Physics, Radboud University/Nikhef, Nijmegen, Netherlands*
- <sup>114</sup>*Nikhef National Institute for Subatomic Physics and University of Amsterdam, Amsterdam, Netherlands*
- <sup>115</sup>*Department of Physics, Northern Illinois University, DeKalb, Illinois, USA*
- <sup>116a</sup>*New York University Abu Dhabi, Abu Dhabi, United Arab Emirates*
- <sup>116b</sup>*United Arab Emirates University, Al Ain, United Arab Emirates*
- <sup>117</sup>*Department of Physics, New York University, New York, New York, USA*
- <sup>118</sup>*Ochanomizu University, Otsuka, Bunkyo-ku, Tokyo, Japan*
- <sup>119</sup>*The Ohio State University, Columbus, Ohio, USA*
- <sup>120</sup>*Homer L. Dodge Department of Physics and Astronomy, University of Oklahoma, Norman, Oklahoma, USA*
- <sup>121</sup>*Department of Physics, Oklahoma State University, Stillwater, Oklahoma, USA*
- <sup>122</sup>*Palacký University, Joint Laboratory of Optics, Olomouc, Czech Republic*
- <sup>123</sup>*Institute for Fundamental Science, University of Oregon, Eugene, Oregon, USA*
- <sup>124</sup>*Graduate School of Science, Osaka University, Osaka, Japan*
- <sup>125</sup>*Department of Physics, University of Oslo, Oslo, Norway*
- <sup>126</sup>*Department of Physics, Oxford University, Oxford, United Kingdom*
- <sup>127</sup>*LPNHE, Sorbonne Université, Université Paris Cité, CNRS/IN2P3, Paris, France*
- <sup>128</sup>*Department of Physics, University of Pennsylvania, Philadelphia, Pennsylvania, USA*
- <sup>129</sup>*Department of Physics and Astronomy, University of Pittsburgh, Pittsburgh, Pennsylvania, USA*
- <sup>130a</sup>*Laboratório de Instrumentação e Física Experimental de Partículas - LIP, Lisboa, Portugal*
- <sup>130b</sup>*Departamento de Física, Faculdade de Ciências, Universidade de Lisboa, Lisboa, Portugal*
- <sup>130c</sup>*Departamento de Física, Universidade de Coimbra, Coimbra, Portugal*
- <sup>130d</sup>*Centro de Física Nuclear da Universidade de Lisboa, Lisboa, Portugal*
- <sup>130e</sup>*Departamento de Física, Universidade do Minho, Braga, Portugal*
- <sup>130f</sup>*Departamento de Física Teórica y del Cosmos, Universidad de Granada, Granada (Spain), Spain*
- <sup>130g</sup>*Departamento de Física, Instituto Superior Técnico, Universidade de Lisboa, Lisboa, Portugal*
- <sup>131</sup>*Institute of Physics of the Czech Academy of Sciences, Prague, Czech Republic*
- <sup>132</sup>*Czech Technical University in Prague, Prague, Czech Republic*
- <sup>133</sup>*Charles University, Faculty of Mathematics and Physics, Prague, Czech Republic*
- <sup>134</sup>*Particle Physics Department, Rutherford Appleton Laboratory, Didcot, United Kingdom*
- <sup>135</sup>*IRFU, CEA, Université Paris-Saclay, Gif-sur-Yvette, France*
- <sup>136</sup>*Santa Cruz Institute for Particle Physics, University of California Santa Cruz, Santa Cruz, California, USA*
- <sup>137a</sup>*Departamento de Física, Pontificia Universidad Católica de Chile, Santiago, Chile*
- <sup>137b</sup>*Millennium Institute for Subatomic physics at high energy frontier (SAPHIR), Santiago, Chile*
- <sup>137c</sup>*Instituto de Investigación Multidisciplinario en Ciencia y Tecnología, y Departamento de Física, Universidad de La Serena, Chile*
- <sup>137d</sup>*Universidad Andres Bello, Department of Physics, Santiago, Chile*

- <sup>137e</sup>*Instituto de Alta Investigación, Universidad de Tarapacá, Arica, Chile*  
<sup>137f</sup>*Departamento de Física, Universidad Técnica Federico Santa María, Valparaíso, Chile*  
<sup>138</sup>*Department of Physics, University of Washington, Seattle, Washington, USA*  
<sup>139</sup>*Department of Physics and Astronomy, University of Sheffield, Sheffield, United Kingdom*  
<sup>140</sup>*Department of Physics, Shinshu University, Nagano, Japan*  
<sup>141</sup>*Department Physik, Universität Siegen, Siegen, Germany*  
<sup>142</sup>*Department of Physics, Simon Fraser University, Burnaby, British Columbia, Canada*  
<sup>143</sup>*SLAC National Accelerator Laboratory, Stanford, California, USA*  
<sup>144</sup>*Department of Physics, Royal Institute of Technology, Stockholm, Sweden*  
<sup>145</sup>*Departments of Physics and Astronomy, Stony Brook University, Stony Brook, New York, USA*  
<sup>146</sup>*Department of Physics and Astronomy, University of Sussex, Brighton, United Kingdom*  
<sup>147</sup>*School of Physics, University of Sydney, Sydney, Australia*  
<sup>148</sup>*Institute of Physics, Academia Sinica, Taipei, Taiwan*  
<sup>149a</sup>*E. Andronikashvili Institute of Physics, Iv. Javakhishvili Tbilisi State University, Tbilisi, Georgia*  
<sup>149b</sup>*High Energy Physics Institute, Tbilisi State University, Tbilisi, Georgia*  
<sup>149c</sup>*University of Georgia, Tbilisi, Georgia*  
<sup>150</sup>*Department of Physics, Technion, Israel Institute of Technology, Haifa, Israel*  
<sup>151</sup>*Raymond and Beverly Sackler School of Physics and Astronomy, Tel Aviv University, Tel Aviv, Israel*  
<sup>152</sup>*Department of Physics, Aristotle University of Thessaloniki, Thessaloniki, Greece*  
<sup>153</sup>*International Center for Elementary Particle Physics and Department of Physics, University of Tokyo, Tokyo, Japan*  
<sup>154</sup>*Department of Physics, Tokyo Institute of Technology, Tokyo, Japan*  
<sup>155</sup>*Department of Physics, University of Toronto, Toronto, Ontario, Canada*  
<sup>156a</sup>*TRIUMF, Vancouver, British Columbia, Canada*  
<sup>156b</sup>*Department of Physics and Astronomy, York University, Toronto, Ontario, Canada*  
<sup>157</sup>*Division of Physics and Tomonaga Center for the History of the Universe, Faculty of Pure and Applied Sciences, University of Tsukuba, Tsukuba, Japan*  
<sup>158</sup>*Department of Physics and Astronomy, Tufts University, Medford, Massachusetts, USA*  
<sup>159</sup>*Department of Physics and Astronomy, University of California Irvine, Irvine, California, USA*  
<sup>160</sup>*University of Sharjah, Sharjah, United Arab Emirates*  
<sup>161</sup>*Department of Physics and Astronomy, University of Uppsala, Uppsala, Sweden*  
<sup>162</sup>*Department of Physics, University of Illinois, Urbana, Illinois, USA*  
<sup>163</sup>*Instituto de Física Corpuscular (IFIC), Centro Mixto Universidad de Valencia - CSIC, Valencia, Spain*  
<sup>164</sup>*Department of Physics, University of British Columbia, Vancouver, British Columbia, Canada*  
<sup>165</sup>*Department of Physics and Astronomy, University of Victoria, Victoria, British Columbia, Canada*  
<sup>166</sup>*Fakultät für Physik und Astronomie, Julius-Maximilians-Universität Würzburg, Würzburg, Germany*  
<sup>167</sup>*Department of Physics, University of Warwick, Coventry, United Kingdom*  
<sup>168</sup>*Waseda University, Tokyo, Japan*  
<sup>169</sup>*Department of Particle Physics and Astrophysics, Weizmann Institute of Science, Rehovot, Israel*  
<sup>170</sup>*Department of Physics, University of Wisconsin, Madison, Wisconsin, USA*  
<sup>171</sup>*Fakultät für Mathematik und Naturwissenschaften, Fachgruppe Physik, Bergische Universität Wuppertal, Wuppertal, Germany*  
<sup>172</sup>*Department of Physics, Yale University, New Haven, Connecticut, USA*

<sup>a</sup>Deceased.

<sup>b</sup>Also at Department of Physics, King's College London, London, United Kingdom.

<sup>c</sup>Also at Institute of Physics, Azerbaijan Academy of Sciences, Baku, Azerbaijan.

<sup>d</sup>Also at Lawrence Livermore National Laboratory, Livermore, USA.

<sup>e</sup>Also at TRIUMF, Vancouver, British Columbia, Canada.

<sup>f</sup>Also at Department of Physics, University of Thessaly, Greece.

<sup>g</sup>Also at An-Najah National University, Nablus, Palestine.

<sup>h</sup>Also at Department of Physics, University of Fribourg, Fribourg, Switzerland.

<sup>i</sup>Also at University of Colorado Boulder, Department of Physics, Colorado, USA.

<sup>j</sup>Also at Department of Physics, Westmont College, Santa Barbara, USA.

<sup>k</sup>Also at Departament de Física de la Universitat Autònoma de Barcelona, Barcelona, Spain.

<sup>l</sup>Also at Affiliated with an institute covered by a cooperation agreement with CERN.

<sup>m</sup>Also at The Collaborative Innovation Center of Quantum Matter (CICQM), Beijing, China.

<sup>n</sup>Also at Department of Physics, Ben Gurion University of the Negev, Beer Sheva, Israel.

<sup>o</sup>Also at Università di Napoli Parthenope, Napoli, Italy.

<sup>p</sup>Also at Institute of Particle Physics (IPP), Canada.

<sup>q</sup>Also at Borough of Manhattan Community College, City University of New York, New York, USA.

<sup>r</sup> Also at National Institute of Physics, University of the Philippines Diliman (Philippines), Philippines.

<sup>s</sup> Also at Department of Financial and Management Engineering, University of the Aegean, Chios, Greece.

<sup>t</sup> Also at Department of Physics, Stanford University, Stanford, California, USA.

<sup>u</sup> Also at Centro Studi e Ricerche Enrico Fermi, Italy.

<sup>v</sup> Also at Institutio Catalana de Recerca i Estudis Avancats, ICREA, Barcelona, Spain.

<sup>w</sup> Also at Technical University of Munich, Munich, Germany.

<sup>x</sup> Also at Yeditepe University, Physics Department, Istanbul, Türkiye.

<sup>y</sup> Also at Institute of Theoretical Physics, Ilia State University, Tbilisi, Georgia.

<sup>z</sup> Also at CERN, Geneva, Switzerland.

<sup>aa</sup> Also at Center for Interdisciplinary Research and Innovation (CIRI-AUTH), Thessaloniki, Greece.

<sup>bb</sup> Also at Hellenic Open University, Patras, Greece.

<sup>cc</sup> Also at Center for High Energy Physics, Peking University, China.

<sup>dd</sup> Also at Department of Physics, Stellenbosch University, South Africa.

<sup>ee</sup> Also at L2IT, Université de Toulouse, CNRS/IN2P3, UPS, Toulouse, France.

<sup>ff</sup> Also at Department of Physics, California State University, Sacramento, USA.

<sup>gg</sup> Also at Département de Physique Nucléaire et Corpusculaire, Université de Genève, Genève, Switzerland.

<sup>hh</sup> Also at Institut für Experimentalphysik, Universität Hamburg, Hamburg, Germany.

<sup>ii</sup> Also at Institute for Nuclear Research and Nuclear Energy (INRNE) of the Bulgarian Academy of Sciences, Sofia, Bulgaria.

<sup>jj</sup> Also at Washington College, Chestertown, Maryland, USA.

<sup>kk</sup> Also at Institute of Applied Physics, Mohammed VI Polytechnic University, Ben Guerir, Morocco.

<sup>ll</sup> Also at Institute of Physics and Technology, Mongolian Academy of Sciences, Ulaanbaatar, Mongolia.

<sup>mmm</sup> Also at University of Chinese Academy of Sciences (UCAS), Beijing, China.